ELSEVIER

Chemical Physics 210 (1996) 297–312

Chemical Physics

Probing the many energy-transfer processes in the photosynthetic light-harvesting complex II at 77 K using energy-selective sub-picosecond transient absorption spectroscopy

H.M. Visser, F.J. Kleima, I.H.M. van Stokkum, R. van Grondelle, H. van Amerongen *

Department of Physics and Astronomy, Vrije Universiteit and Institute for Molecular and Biological Sciences, De Boelelaan 1081, 1081 HV Amsterdam, The Netherlands

Received 2 January 1996

Abstract

The dynamics of energy equilibration in the main plant light-harvesting complex, LHCII, at a temperature of 77 K was probed using sub-picosecond excitation pulses at 649, 661, 672 and 682 nm and detection of the resulting difference absorption spectra from 630 to 700 nm. We find three distinct chlorophyll *b* to chlorophyll *a* (Chl *a*) transfer times, of < 0.3, 0.6 and 4–9 ps, respectively. From a comparison of the amplitudes of the bleaching signal, a plausible scheme for the Chl *b* to Chl *a* transfer in the LHCII complex is proposed. Two Chl *b* molecules transfer energy to Chl *a* in less than 0.3 ps, two Chl *b* molecules transfer with 0.6 ps and one Chl *b* has a transfer time of 4–9 ps. In the Chl *a* absorption region, a 2.4 ps energy-transfer process from a pigment absorbing around 661 nm, and a 0.4 ps process from a pigment absorbing around 672 nm is found. Furthermore, evidence is found for slow, 10–20 ps energy-transfer processes between some of the Chl *a* molecules. The data are compared to model calculations using the 3.4 Å LHCII monomer structure (containing 5 Chl *b* and 7 Chl *a* molecules) and Förster energy transfer. We conclude that the observed energy-transfer rates are consistent with both the preliminary assignment of the Chl identities (*a* or *b*) of Kühlbrandt et al. and a recent proposal for the arrangement of some of the transition dipole moments (Gülen et al.). Singlet–singlet and singlet–triplet annihilation processes are observed in two different experiments, and both these processes occur with time constants of 2–3 and 12–20 ps, suggesting that both annihilation pathways are at least partly limited by slow energy transfer. The wide range of observed time constants in the equilibration, from < 0.3 to ~ 20 ps, most likely reflects the irregular arrangement of the pigments in the complex, which shows much less symmetry than the recently obtained structure of the peripheral antenna complex of purple bacteria, LH-II (McDermott et al.).

1. Introduction

In leaves, more than 50% of the light is absorbed by the main plant light-harvesting antenna complex, LHCII [1]. Excited-state energy is transferred from this trimeric complex of approximately 80kDa to the reaction center core of mainly photosystem II. The protein contains Chl *b*, Chl *a* and carotenoids as its pigments, thus absorbing light over a wide range in the visible spectrum. In addition to their role as light-harvesting pigments, carotenoids are useful as

* Corresponding author. Fax: +31 20 4447899; E-mail: herbert@nat.vu.nl.

PII S0301-0104(96)00092-4

quenchers of chlorophyll triplets, thus lowering the yield of harmful singlet oxygen production [2]. The model of the crystal structure of LHCII was recently refined to a resolution of 3.4 Å [3]. In this structure twelve chlorophyll molecules and two carotenoids (presumably luteins) were resolved per monomeric subunit. The protein backbone, consisting of 125 residues, contains three transmembrane helices. The luteins are located in the central part of each monomer, which seems to be held together by these pigments. From the present structural data Chl *a* and Chl *b* cannot be identified and the orientations of the lowest-energy electronic transition dipole moment (Q_y transition) in each of the chlorophylls cannot yet be assigned. In a preliminary assignment, the seven molecules closest to the luteins were proposed to be Chl *a*, the remaining five chlorophylls then were suggested to be Chl *b*. Given this assignment it is possible to deduce the orientations of the transition dipole moments of several chlorophylls [4]. The LHCII complex has extensively been studied spectroscopically, both with steady-state [5–10] and time-resolved techniques [11–19]. Whereas only two main absorption bands in the 640–700 nm region are observed at room temperature, as many as 6 to 9 bands were observed in absorption, circular dichroism and linear dichroism spectra of the complex at 77 K [5] and today the spectral fingerprint of LHCII consists of eleven features [7]. Several (sub)-picosecond spectroscopic studies have been performed on LHCII, mostly at room temperature. A pioneering fluorescence upconversion study by Eads et al. [11] revealed that the dominant time constant for energy transfer from Chl *b* to Chl *a* was 0.5 ± 0.2 ps in a strain of *C. reinhardtii*, which is devoid of photosystem I and II. A subsequent low-intensity transient absorption study with an instrument response function of 3–4 ps (FWHM) revealed besides unresolvably fast sub-ps transfer times also slower transfer times (2–6 ps), both for Chl *b* to Chl *a* and for Chl *a* to Chl *a* transfer [12]. Even slower processes (14–36 ps) were observed that were probably mainly due to singlet–triplet annihilation. A recent transient absorption study using 130 fs pump and probe pulses arrived at lifetimes of 160 ± 20 fs and 5 ± 2 ps upon excitation of mainly Chl *b* at 645 nm and detection at 655 nm and similar rise times were observed at 680 nm, thus reflecting energy transfer from Chl *b* to Chl *a* [16]. Singlet–singlet annihilation was found to set in at $\sim 4 \times 10^{14}$ photons cm^{-2} per pulse. At room temperature, singlet–singlet annihilation appears as a decay of the 680 nm bleaching with a ~ 20 ps time constant. No annihilation between Chl *b* pigments could be observed, even at intensities up to $\sim 6 \times 10^{15}$ photons cm^{-2} per pulse. In a fluorescence upconversion study by Du et al. [14], two lifetimes in the rise of presumably the Chl *a* fluorescence were detected upon excitation at 650 nm: ~ 250 fs and 5 ps, in rather good agreement with findings mentioned earlier. However, interpretation of the results was complicated by the spectral overlap of Chl *a* and Chl *b* fluorescence. In a one-color transient absorption study of Pålsson et al. [15], a decay time of 0.5 ± 0.2 ps was observed upon excitation at 650 nm and this time was assigned to Chl *b* to Chl *a* transfer. The same experiment furthermore yielded a 2 ps decay time at this wavelength (relative contribution 20%). Despite the 100 fs time resolution of the experiment no transfer times could be resolved that were shorter than 0.5 ± 0.2 ps. Excitation at 665 nm led to a 20% contribution of a 2 ps component and a 80% contribution of a 10–20 ps component. Similar times were observed by Kwa et al. [12] after excitation at 665 nm but the relative contribution of these components was reversed. In the 3.4 Å model of LHCII, 12 chlorophylls were observed but their identity could not be deduced from structural data [3]. The seven chlorophyll molecules that were located besides the central carotenoids were assigned to Chl *a* and the remaining five were assigned to Chl *b*. Amongst others this assignment was based on the argument that carotenoids in LHCII can only function as quenchers of triplet states (which mainly originate on Chl *a* pigments) if they are in close contact with these molecules. In a recent study in our group we could only find evidence for contacts between Chl *a* and carotenoids but we could not exclude that some Chl *b* molecules might be located very close to some carotenoids [20]. Taking this assignment, the center to center distances between Chl *a* and Chl *b* range from 8.3 to 10.5 Å. Kühlbrandt et al. [3] concluded that this assignment is in agreement with a 0.5 ps transfer time from Chl *b* to Chl *a*. In sharp contrast with this assignment is the suggestion by Pålsson et al. [15] that Chl *b* and Chl *a* molecules are separated into two different

levels of pigments that were already observed in the 6 Å model of LHCII [1]. Also a few low-temperature studies have been performed. In a polarized transient absorption experiment Savikhin et al. [18] observed that the depolarization at 680 nm occurs with a time constant of 5 ps at room temperature and slows down to 34 ps at 12 K. Since the residual anisotropy increases upon lowering the temperature it seems that a fraction of the excited states gets virtually trapped on the time scale of the experiment (several hundreds of picoseconds). In a study by Bittner et al. [17] LHCII at 12 K was excited at 640 nm. Rise times of 340 fs and 1 ps were observed in the Chl *a* Q_y region. Moreover, spectral equilibration in the Chl *a* Q_y region was observed with a time constant of 14 ps, whereas annihilation took place on a time scale of approximately 500 ps. In a fluorescence photon counting experiment at 80 K on trimeric LHCII an energy-transfer process of 13 ps was observed as a rise of the fluorescence above 680 nm after excitation at 665 nm [13].

Whereas it is generally agreed upon that the spread in energies and distances between the pigments will lead to a multitude of lifetimes in the equilibration of the energy in LHCII, so far most experimental studies detected only a limited number of decay components. In this study we present subpicosecond transient absorption measurements on LHCII at 77 K, using spectrally well defined (~ 5 nm FWHM) excitation pulses at 4 different wavelengths: 649, 661, 672 and 682 nm. The entire Q_y region was probed simultaneously after excitation of both Chl *a* and Chl *b*. The results allow us to find direct evidence for four lifetimes, whereas the presence of at least two other lifetimes can easily be deduced. The results are interpreted in terms of the 3.4 Å model of LHCII [3] with the use of Förster energy-transfer calculations [21]. A preliminary report about part of the data was given elsewhere [19].

2. Materials and methods

LHCII complexes were isolated following a novel procedure, shortly described in Ref. [20]. Samples were dissolved in 65–75% glycerol (v/v) for low-temperature measurements. The sample was placed in acrylic cuvettes with a pathlength of 1 mm in a liquid nitrogen cryostat (Oxford Instruments DN1704). To obtain difference spectra with sub-picosecond time resolution, a femtosecond spectrophotometer was used as described previously [22], with some minor modifications. The continuum was created by weakly focusing pump and probe beams (center wavelength ~ 650 nm, ~ 100 μJ/pulse, ~ 0.8 cm diameter) in a 2 mm thick sapphire plate (Melles–Griot). The resulting continuum appears spectrally more stable than the continuum created in water. Using 1 mm thin interference filters with a spectral width of ~ 5 nm FWHM (Ferroperm, Vedbaek, Denmark), a desired excitation wavelength was selected and amplified by a single pass through a flowed dye cuvette. Noise in the resulting pump pulse energies was 5–10% rms. Pump and probe beam were focused in the sample by a 15 cm lens. Diameters of pump and probe spot were estimated at ~ 0.1 mm, the pump energy at the sample was 0.1 μJ typically, resulting in an excitation density of 4×10^{15} photons cm^{-2} per pulse. Group velocity dispersion (GVD) compensation in the excitation beam was achieved by two SF-10 prisms at 45 cm separation to remove any chirp on the excitation pulses. The instrument response width was estimated by a global analysis routine [23]. Values ranging from 0.28 ps (FWHM) for the 649 nm excitation dataset to 0.37 ps for the 661 nm excitation dataset were found, approximating the instrument response function by a Gaussian shape in the fitting routine. The instrument response may be compared with the Fourier transform limit: for a Gaussian pulse at 649 nm with a width of 4.4 nm as used in the experiments (see Fig. 1), one calculates a transform-limited pulsewidth of 156 fs. Since the probe light has a much wider spectrum, this number represents the minimum response time ideally achievable. Thus, the experimental instrument response is within a factor of two of the theoretical limit. Time zero ($t = 0$), defined as the moment of maximum temporal overlap between pump and probe pulses, was estimated by the global analysis routine. A linear dependence of the initial bleaching signal (~ 0.5 ps after $t = 0$) on the pump energy was observed by varying the excitation density from 30 to 200% of the value used in the measurements shown. Noise in the spectra is typically 3×10^{-3} as estimated from the baseline

taken well before $t = 0$ (see e.g. Fig. 3a). Data collection procedures were as described before [22].

For single-color pump–probe measurements, pulses from a Coherent MIRA Ti : sapphire were amplified at 50 or 200 kHz in an Ar-ion laser pumped Ti : sapphire regenerative amplifier (Coherent RegA 9000). A part of the white light from a continuum created by the ~ 4 μJ, ~ 800 nm pulses was amplified in an optical parametric amplifier (OPA). In this way, ~ 50 nJ pulses around 650 or 680 nm were obtained. Again, a ~ 5 nm FWHM interference filter was used to shape the excitation spectrally. Part of the same beam was split off by a beam splitter and used as a probe beam. In the measurements shown (the excitation pulse energy was 0.8 nJ typically) the beam was focused in a focal spot with an estimated diameter of ~ 35 μm, resulting in an excitation density of 2×10^{14} photons cm^{-2} per pulse, roughly 20 times lower than in the multi-color detection setup. Again, a linear dependence of the initial bleaching signal on the excitation pulse energy was observed. The pump beam was modulated at approximately 1 kHz and the resulting modulation on the probe beam was detected through a lock-in amplifier. Kinetic curves consisted of 400 points, taken with 1 s averaging per time point. Subsequent scans were identical within the noise. The instrument response was measured by taking the cross correlation between pump and probe at the sample position. Instrument response widths of 0.24 and 0.20 ps were found for the 650 and 680 nm excitation experiments in Fig. 2, respectively. All transient absorption measurements shown were performed with the probe light at magic angle (54.7°) with respect to the pump light.

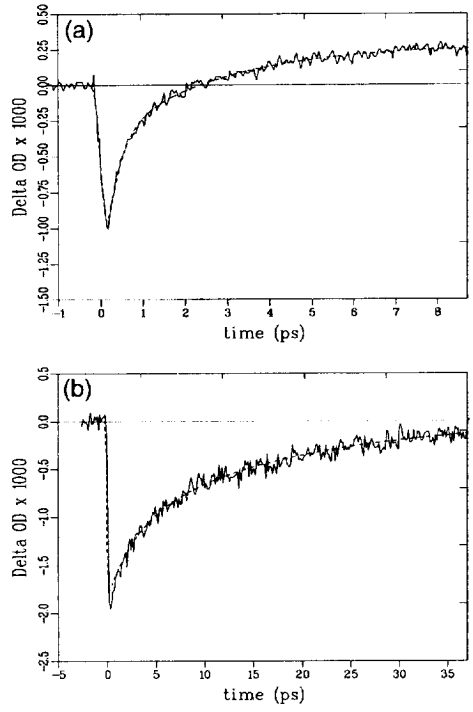

Fig. 2. (a) Single-color pump–probe signal at low intensity (approximately 2×10^{14} photons cm^{-2} per pulse) with both excitation and detection at 650 nm, in the Chl *b* absorption band (see Fig. 1) of LHCII at 77 K. Dashed line: bi-exponential fit. $\tau_1 = 0.31$ ps, $\tau_2 = 2.6$ ps. $A_1 = 61\%$, $A_2 = 39\%$. (b) Single-color pump–probe signal at low intensity (approximately 2×10^{14} photons cm^{-2} per pulse) with both excitation and detection at 680 nm, on the low-energy side of the Chl *a* absorption band (see Fig. 1) of LHCII at 77 K. Dashed line: bi-exponential fit. Dashed line: bi-exponential fit. $\tau_1 = 2.9$ ps, $\tau_2 = 17$ ps. $A_1 = 38\%$, $A_2 = 62\%$.

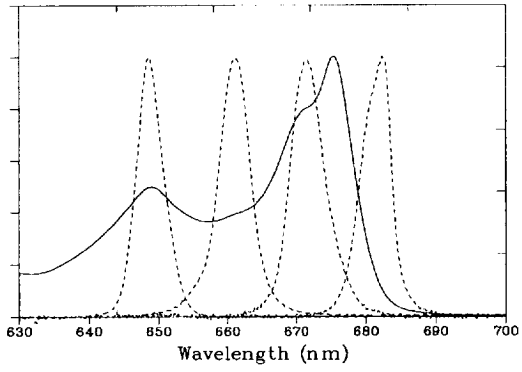

Fig. 1. Absorption spectrum of LHCII at 77 K (solid) and spectra of the excitation pulses used (dashed). The width of the excitation spectrum varies from 4.4 nm (FWHM) upon 649 nm excitation to 5.5 nm upon 672 nm excitation.

3. Results

The absorption spectrum of the LHCII preparations at 77 K as used in the measurements is shown in Fig. 1. Also shown are spectra of the excitation pulses. Excitation at 649 nm mainly results in excited Chl *b* molecules, while at 661, 672 and 682 nm the major part of the absorption is due to Chl *a*. As a first result we show in Fig. 2a a low-intensity

single-color pump–probe kinetic trace measured with excitation and detection at 650 nm. In reasonable agreement with results obtained under similar conditions at room temperature [15] we find that a 0.3 ± 0.1 ps lifetime dominates the kinetics, most likely reflecting transfer from Chl *b* to Chl *a*. For a satisfactory description of the data, a second lifetime τ_2 of 2.6 ± 0.7 ps has to be included in the fit. The dashed line indicates the best fit to the data using bi-exponential decay, with lifetimes $\tau_1 = 0.31$ ps and $\tau_2 = 2.6$ ps and amplitudes $A_1 = 61\%$ and $A_2 = 39\%$.

A non-decaying offset (of -16%) was also included. A convolution of this decay function with a Gaussian instrument response (FWHM 0.20 ps) was performed. The signal is negative for delays longer than 2.4 ps, indicative of excited state absorption of Chl *a* molecules, similar to the observation reported by e.g. Kwa et al. [12] for LHCII at RT. Fig. 2b shows the results from a similar experiment with excitation and detection at 680 nm, on the low-energy side of the Chl *a* absorption (see Fig. 1). This signal decays, most likely due to singlet–triplet annihilation, with time constants of 2.9 and 17 ps, corresponding amplitudes were $A_1 = 38\%$ and $A_2 = 62\%$, respectively. To monitor the spectral changes over a broad range of detection wavelengths upon selective excitation, we used the spectrophotometer described above. Fig. 3 shows some typical transient absorption difference spectra obtained upon excitation at 649 nm. The presented transient absorption spectra were taken with a delay of 0.35 ps in the first spectrum up to 45.3 ps for the last spectrum (Fig. 3a). Several dynamic processes are immediately visible in the raw data. The bleaching/stimulated emission (SE) around 650 nm decays on a sub-picosecond time scale concomitant with a growth of the bleaching/SE around 679 nm, reflecting energy transfer from Chl *b* to Chl *a*. On a ~ 20 ps time scale, this bleaching/SE around 679 nm decays, most likely due to singlet–singlet annihilation. The total data set containing 32 transient spectra was analyzed using a global analysis routine [23]. In addition to the instrument response parameters at least four lifetimes are needed to obtain a satisfactory fit and three of the resulting decay-associated (D-A) spectra are shown in Fig. 3b. The lifetimes associated with these spectra are 0.62, 12 and 260

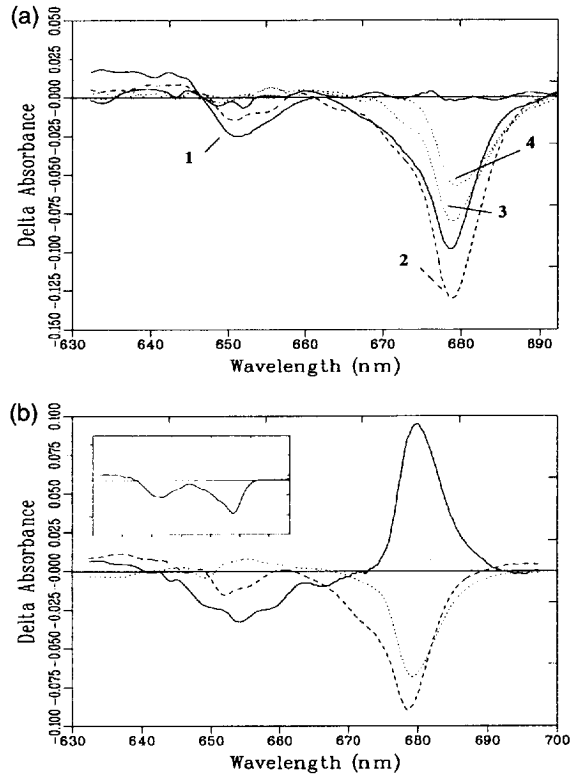

Fig. 3. (a) Difference spectra of LHCII at 77 K after excitation at 649 nm, clearly showing transfer from Chl *b* around 650 nm to Chl *a* around 679 nm. Spectra 1–4 were taken at $t = 0.35$, 1.85, 16.4 and 45.3 ps, respectively. Also shown is a baseline as measured well before $t = 0$ (solid). (b) Decay-associated (D-A) spectra obtained from a global analysis of the dataset from which the spectra in (A) were taken. Lifetimes associated with these spectra: 0.62 ps (solid) and 12 ps (dashed). Also a non-decaying component is found (i.e. > 200 ps in this case, dotted). The inset shows the sum of the three D-A spectra presented, over the same wavelength interval.

ps, respectively. Not shown is a spectrum with a lifetime of 0.14 ps, significantly shorter than the instrument response width. The spectrum associated with the longest lifetime (dotted) is essentially non-decaying on the time scale of the measurement (45 ps) and shows that the excitation becomes localized on Chl *a*. It peaks at 679 nm, 3 nm to the red of the major Chl a absorption peak. A 3 nm red shift of the former peak with respect to the absorption peak seems reasonable. From a hole-burning study on LHCII it was deduced that the lowest energy state is located at 680 nm and it gives rise to fluorescence

(and thus stimulated emission) with a peak at 681 nm [10]. If all excitations would localize on the lowest energy state (which might happen at 4 K) the maximum of the bleaching/SE would be located at 680.5 nm, but since at 77 K also higher-energy states will be populated the actual maximum will be located slightly to the blue. This population of higher-energy states probably also explains why we do not observe bipolar signals in the Chl a region like Bittner et al. [17] at 12 K. In general, the maximum of the bleaching/SE peak will be located to the red of the position of the corresponding absorption transitions. The spectrum associated with the 0.6 ps time constant (solid line) shows an S-shape typical for energy transfer, in this case from Chl *b* to Chl *a*. The 12 ps spectrum (dashed) reflects loss of bleaching/SE in the Chl *a* region, most likely due to singlet–singlet annihilation. Notice that the 12 ps spectrum is clearly different from the non-decaying spectrum: a shoulder at ~ 670 nm is present in the 12 ps spectrum which is absent in the non-decaying spectrum. Furthermore, the 12 ps spectrum suggests that a fraction of the decay of the Chl *b* takes place with a 12 ps time constant (but see also below). This shows that a fully equilibrated state has not yet been reached when the annihilation process sets in, indicating the occurrence of relatively slow energy-transfer processes. One lifetime (0.14 ps) obtained from the global analysis is significantly shorter than the instrument response width. To assess the amount of fast, unresolved Chl *b* to Chl *a* transfer, we show the sum of the three slower D-A spectra as an inset in Fig. 3b, representing the ΔOD spectrum after the unresolvably fast processes. From this spectrum, we estimate that due to these ultrafast processes, already 54% of the excitations is localized on Chl *a*. This is significantly more than the amount expected from direct absorption of Chl *a* via the vibrational side band, and we estimate that 34% of the excitations created upon excitation at 649 nm is transferred with a time constant of < 0.3 ps, and 20% of the excitation corresponds to direct excitation of Chl *a* which is in agreement with estimates by other authors [16,11]. This estimation was done by comparing the LHCII absorption with that of Chl *a* in LHCII. In the Appendix it is described how the absorption spectrum of Chl *a* in LHCII at 77 K is approximated. The slow energy-transfer process of ~ 3 ps

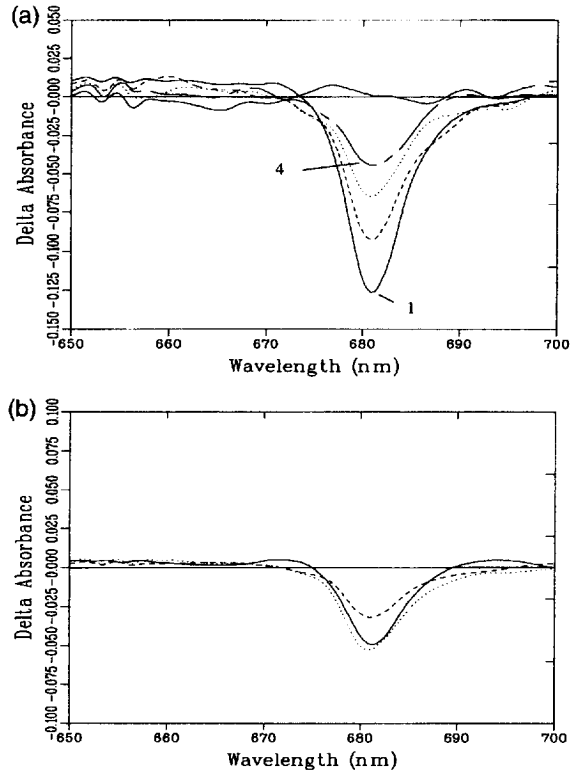

Fig. 4. (a) Difference spectra of LHCII at 77 K after excitation at 682 nm. The signal decreases with time, but no large spectral changes occur. Spectra 1–4 were taken at $t = 0.23$, 2.1, 20.7 and 671 ps, respectively. Also a baseline as measured well before $t = 0$ (solid) is shown. (b) D-A spectra obtained from a global analysis of the dataset from which the spectra in (A) were taken. Lifetimes associated with these spectra: 1.9 ps (solid) and 20 ps (dashed). Also a non-decaying component is found (i.e. > 1 ns in this case, dotted).

that was detected in the one-color experiment at 650 nm (see above) is not observed as a transfer process from Chl *b* to Chl *a* after global analysis of the data. This is probably due to the fact that annihilation between Chl *a* molecules is occurring and this is fitted with a 12 ps component. The large corresponding amplitude of this process in the Chl *a* region forces also the slow decay in the Chl *b* region to be fit with the same time constant. Global analysis of the data in the Chl *b* wavelength region alone leads to a decay time of 7 ± 3 ps.

Fig. 4a shows transient absorption spectra from a dataset obtained with excitation at 682 nm. At first sight no clear signs of energy transfer are visible in

these spectra, but again annihilation can be observed. Fig. 4b shows the decay-associated spectra for this dataset that extends to a maximum delay of 670 ps. Note that the shape of all three spectra is similar, quite unlike the case of 649 nm excitation shown in Fig. 3a. Lifetimes of 1.9 and 20 ps are found besides a non-decaying component (lifetime estimated at 3.3 ns by the fitting routine). The 20 ps lifetime is similar to the 12 ps lifetime observed upon excitation at 649 nm, and also in this case most likely results from singlet–singlet annihilation, since the spectrum reflects a loss of bleaching/SE. The 1.9 ps spectrum also corresponds to a loss of bleaching/SE and probably partly reflects a fast phase in the annihilation process that is not observed upon excitation at 649 nm but the spectrum also shows some signs of energy transfer towards states at higher and lower energy. We did similar experiments at three-fold higher energies which gave rise to a strong increase of the amount of annihilation. Similar D-A spectra were obtained and the corresponding times were approximately 0.5 and 18 ps. We also performed single-color transient absorption measurements at 680 nm (Fig. 2b) where the intensity per shot was much lower so that no significant amount of singlet–singlet annihilation could take place but the repetition frequency was high enough to ensure the occurrence of singlet–triplet annihilation (see also Peterman et al. [20]). Surprisingly, in these experiments similar time constants were found: 2.9 and 17 ps, indicating that the annihilation process is probably excitation transfer limited. It may be noted that the initial bleaching in Fig. 4a is narrower than the final bleaching: 5.5 versus 7.5 nm FWHM respectively. During the in-growth of the transient absorption difference spectrum (from $t = -0.2$ to 0.2 ps) the maximum of the signal shifts from 679 to 682 nm. This is at least partly due to vibrational relaxation in the excited state. Apparently, the broad laser pulse initially leads to preferential excitation more to the blue where the absorption is higher than at 682 nm.

In Fig. 5a some typical spectra upon excitation at 661 nm are shown. This dataset extends to 45 ps. The initial bleaching/SE spectra are clearly wider than those observed upon excitation at 682 nm. Concomitant with an instantaneous bleaching/SE around 664 nm, a bleaching/SE signal at 678 nm is observed. With increasing delay time the bleaching

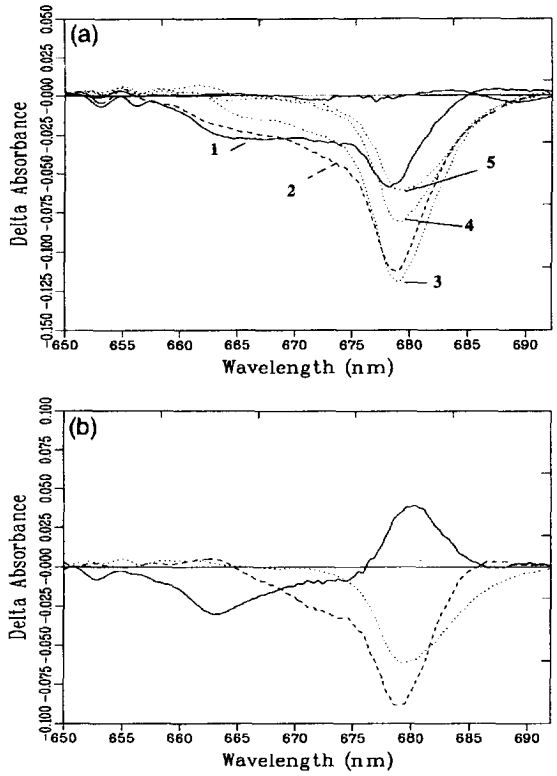

Fig. 5. (a) Difference spectra of LHCII at 77 K after excitation at 661 nm. Energy transfer on a picosecond time scale from ~ 664 to ~ 679 nm is visible. Spectra 1–5 were taken at $t = 70$ fs, 0.49, 2.7, 16.2 and 36.9 ps respectively. Also shown is a baseline as measured well before $t = 0$ (solid). (b) D-A spectra obtained from a global analysis of the dataset from which the spectra in (A) were taken. Lifetimes associated with these spectra: 2.4 ps (solid) and 12 ps (dashed). Also a non-decaying component is found (i.e. > 200 ps in this case, dotted).

around 664 nm decays while the 678 nm bleaching continues to increase. At longer time delays the bleaching at 664 nm has fully disappeared, and the bleaching at 678 nm decays. Results from the global analysis (Fig. 5b) clearly show a 2.4 ps energy-transfer component (solid line in Fig. 5b) from 663 to 679 nm, and a 12 ps decay of bleaching (dashed) strongly reminiscent of the decay attributed to singlet − singlet annihilation in the previous two datasets. Again the corresponding decay-associated spectrum shows a shoulder around 670 nm. A similar non-decaying spectrum (dotted) as in the previous sets is found. As in the case of 649 nm, a process faster than the

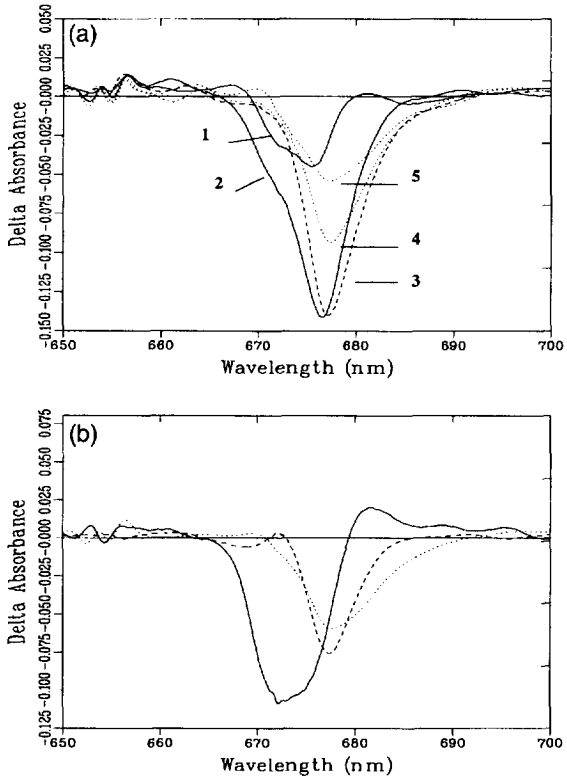

Fig. 6. (a) Difference spectra of LHCII at 77 K after excitation at 672 nm. In this case, energy transfer from ~672 to ~678 nm is visible in the data as a narrowing of the ΔOD spectrum. Spectra 1–5 were taken at $t = 0$ fs, 0.25, 1.0, 12.6 and 271 ps respectively. (b) D-A spectra obtained from a global analysis of the dataset from which the spectra in (A) were taken. Excitation was at 672 nm. Lifetimes associated with these spectra: 0.42 ps (solid), 18 ps (dashed) and non-decaying (i.e. > 0.5 ns, dotted).

instrument response may be present in the data; the fitting routine finds a 0.13 ps component which has partly an energy-transfer character (from 665 to 679 nm, spectrum not shown). However, a large part of the pigments absorbing above 670 nm has been excited directly via their vibrational bands, and the observed ultrafast transfer from 665 to 679 nm could also partly reflect vibrational relaxation.

In Figs. 6a and 6b we show results of a similar experiment with excitation at 672 nm and a maximum delay time of 271 ps. Some structure in the spectra around 650 nm, most visible in Fig. 6, we attribute to some instability in the continuum at the center wavelength of the generating pulses. The initial bleaching spectra are narrower than in the case of 661 nm excitation (Fig. 5), but wider than upon excitation at 682 nm (Fig. 4). The spectra from the global analysis are associated with lifetimes of 0.42 ps, 18 ps and a non-decaying spectrum (fitted lifetime 2.6 ns). The 0.42 ps spectrum (solid line in 6b) shows clear signs of energy transfer to longer wavelength bands, but it also indicates an overall loss of bleaching/SE (possibly annihilation). Again we ascribe the loss of bleaching represented by the 18 ps decay-associated spectrum (dashed) to singlet–singlet annihilation. The non-decaying spectrum (dotted) is again similar to the non-decaying spectra found in the other datasets.

In summary, in the multi-color experiments on LHCII at 77 K we

- directly observe down-hill energy-transfer processes with time constants of 0.6, 2.4 and 0.4 ps upon selective excitation at 649, 661 and 672 nm, respectively. In all cases transfer is directly to states which lead to bleaching/SE signals near 679 nm,
- deduce from the data that a fast Chl $b \rightarrow$ Chl a transfer time (< 300 fs) is obscured by the 0.3 ps instrument response upon excitation at 649 nm. Upon excitation at 661 nm, some fast (< 0.3 ps) energy transfer may take place,
- deduce the presence of a minor fraction of slow (4–9 ps) Chl b to Chl a transfer,
- deduce from the data that slow (~ 10–20 ps) energy transfer within the Chl a pool takes place,
- find that at the excitation density used (4×10^{15} photons cm^{-2} per pulse) annihilation results in a reduction of the bleaching of ~ 40% with a time constant of 12–20 ps,
- upon direct excitation of the lowest-energy absorption band, an additional 2 ps phase in singlet–singlet and singlet–triplet annihilation is observed.

4. Discussion

4.1. Excitation of Chl b at 650 nm results in 3 different time constants for energy transfer

Upon excitation of Chl b at 649 nm, we observe, in the multi-color experiments a decay of the Chl b bleaching with a 0.6 ps time constant and a slower,

4–9 ps time constant. The multi-color experiment shows that the 0.6 ps process reflects energy transfer to a state which gives rise to a peak near 679 nm. From the ΔOD spectrum extrapolated back to a moment in time before these two processes set in (where the excitation has taken place and the fastest process is already over) as shown in Fig. 3b, we conclude that a fast, < 300 fs Chl *b* to Chl *a* transfer process must be present as well. After correction for direct excitation of Chl *a* (see above) and assuming that all the Chl *b* have the same absorption spectrum, we estimate the relative amplitudes of these processes from the data to correspond to approximately 42, 41 and 17% for the two faster (< 300 and 600 fs) and the slower process (4–9 ps), respectively. The one-color transfer from 650 nm was satisfactorily fit with two decay times of 0.3 and 2.6 ps. However, a three-exponential fit gave results more similar to those from the multi-color experiments as reflected by the decay times of 100 fs, 500 fs and 3.1 ps. The relative amplitudes are 37, 33 and 29%, respectively. The observed time constants are in good agreement with previous work. A < 300 fs process was observed by Bittner et al. [16,17] and Du et al. [14] in transient absorption and fluorescence upconversion studies, respectively. Eads et al. [11] and Pållsson et al. [15] reported a 500 fs process upon excitation at 650 nm. All these studies used different ways for determining the transfer rates and probably different time constants were projected out in each of these particular experiments. We have for the first time now found evidence for the coexistence of several transfer processes from Chl *b* to Chl *a* on a sub-picosecond time scale with different time constants and we have determined their relative contributions. Energy-transfer processes from Chl *b* to Chl *a* that are slower than 1 ps were also reported before by Kwa et al. [12], Bittner et al. [17], Pålsson et al. [15] and Du et al. [14]. We now conclude that most likely one out of five Chl *b* molecules is responsible for such a relatively slow energy transfer. The atomic model of LHCII as determined by Kühlbrandt et al. [3] shows 5 Chl *b* molecules per monomer. It thus appears that two Chl *b* molecules transfer their energy ultrafast (< 300 fs) to Chl *a*, two have time constants of ~ 0.6 ps and one transfers its energy much slower, i.e. in 4–9 ps. Below we will investigate whether the data can be explained within the context of the current assignment of the Chl identities.

In the early-time spectra, upon excitation at 649 nm, we noticed short-lived excited state absorption on the high-energy side of the Chl *b* absorption (see Fig. 3a). This feature may be indicative of excited state absorption due to exciton coupling between two Chl *b* molecules [24]. Note that circular dichroism measurements indicate the presence of excitonic interactions between Chl *b* molecules [7]. It has been proposed in the literature that a Chl *b* exciton state is present near 665 nm (coupled to two 652 nm states) which would function as an intermediate for energy transfer from Chl *b* to Chl *a* [6,25–27]. Our present results do not support this proposal. The absorption around this wavelength is largely due to vibronic bands of longer wavelength Chl *a*. Superimposed on this is a distinct absorption band, which is discernible at 77 K (see Fig. 1) but which has a dipole strength of approximately one Chl *a* molecule. Excitation in this band (662 nm) leads to a significant amount of direct excitation of longer wavelength pigments via the vibronic bands, but also a 2.4 ps transfer can be distinguished which reflects energy transfer from the 662–665 nm state. The question now is whether this is a Chl *b* exciton state or a Chl *a* state. However, it turns out that after excitation in the main Chl *b* band (Fig. 3) transfer does not proceed via this 662 nm state since no spectral components are observed near this wavelength with a lifetime of several picoseconds.

4.2. Equilibration between Chl a molecules takes place with sub-picosecond to picosecond time constants

For both datasets with excitation at 649 and 661 nm, it can be observed that equilibration among the Chl *a* pigments in LHCII is not complete when singlet–singlet annihilation sets in. This is apparent from the D-A spectrum of the 12 ps components in Figs. 3b and 5b, which both show a pronounced shoulder around 670 nm which is absent in the non-decaying spectrum. Thus, part of the energy transfer from 670 to 676 nm must be slow (> 10 ps) which seems to be in agreement with an observed spectral equilibration time in the Chl *a* pool of 14 ps at 12 K [17]. In our case this slow phase in the

equilibration cannot be observed directly since annihilation gives rise to a decay of the bleaching on a 2–20 ps time scale. However, upon excitation at 672 nm, this slowly transferring state is not populated by the exciting laser pulse directly since in the case only a fast 0.4 ps energy-transfer process is observed. Thus it appears that around 672 nm a pigment absorbs that transfers its energy within one picosecond to a longer wavelength state. Upon excitation at 662 nm, a 2.4 ps D-A spectrum was found that may correspond to a pigment absorbing around 662 nm and transferring excitations either to ~ 676 nm or to ~ 672 nm (in the latter case the excitation is quickly transferred to pigments absorbing around 676 nm, as was already concluded above). A similar time constant of 2 ps was observed by Kwa et al. [12] upon excitation at 660 and 665 nm.

4.3. Annihilation occurs with 2–3 and 12–20 ps time constants and may be partly limited by energy transfer

In all datasets shown in Figs. 3 to 6 we observe a distinct decay of the induced bleaching with a 12–20 ps time constant. In all four experiments, the maximum bleaching reached at 679 nm was the same to within 20%. Thus, annihilation in all four cases is expected to be similar. Indeed, comparable time constants and amplitudes are found. Similar time constants were observed by Bittner et al. [16] who used similar excitation densities on LHCII at RT. Upon excitation at 682 nm however, an additional 1.9 ps time constant is found. This component is not observed upon excitation at other (shorter) wavelengths, probably due to energy-transfer processes occurring on a similar or even slower time scale. A tempting explanation for the two annihilation phases is that the 1.9 ps component arises from singlet–singlet annihilation within LHCII monomers, whereas the 12–20 ps component arises from annihilation between excitations originally on different monomers. To study this possibility, experiments on LHCII monomers, that recently became available [7], will be worthwhile. It is striking that the singlet–triplet annihilation observed in the lower-intensity experiment (Fig. 2b) occur with so similar time constants (3 and 17 ps). This seems to point at a situation in which both singlet–singlet and singlet–triplet annihilation are energy transfer limited. Finally we note that the singlet–triplet annihilation appears to be remarkably efficient: on a 40 ps time scale, the induced bleaching almost completely decays to zero. At 77 K, it is more difficult to avoid singlet–triplet annihilation than at room temperature, since each shot leads to a small fraction of long-lived Chl a triplets, which are not being quenched at 77 K, in contrast to room temperature conditions [20].

Table 1
Overview of observed processes in LHCII

Process	t (ps)	from (nm)	to (nm)
EET	< 0.3	650 (~ 40%)	679
EET	0.6	650 (~ 40%)	679
EET	4–9	650 (~ 20%)	679
EET	2	662	679
EET	10–20	670	679
EET	0.4	672	679
S–S annihilation	2	–	–
S–S annihilation	12–20	–	–
S–T annihilation	3	–	–
S–T annihilation	17	–	–

EET denotes excitation energy transfer, the S stands for singlet, T for triplet.

Table 1 contains an overview of the various energy-transfer processes observed in LHCII in these experiments.

4.4. Modelling energy transfer by a Förster mechanism

Whether or not energy transfer within LHCII can be modelled by the Förster mechanism has been an open question since the first ultrafast studies were performed on this complex [11]. With distances between the Chl *a* molecules of 8 Å and $\kappa = 1$, the excitonic dipole coupling between two Chl *a* molecules in the complex can be as large as 180 cm^{-1} assuming a value of 1 for the refractive index n (for the definition of κ, see the Appendix). A more typical value, found for a distance of 11 Å, is 70 cm^{-1} which reduces to less than 20 cm^{-1} for a value of $n = 2$. Since the Chl *b* (650 nm) and Chl *a* (676 nm) absorption are separated by almost 600 cm^{-1}, no Chl *a* exciton bands are expected to contribute to the absorption in the Chl *b* region, around 650 nm. Therefore, excitation at 649 nm

either excites Chl *b* or directly excites Chl *a* via vibrational bands. Similarly, the strongest coupling between Chl *b* and Chl *a* pigments are at most 140 cm^{-1} (or 35 cm^{-1} for $n = 2$). Therefore, interactions between Chl *b* and Chl *a* molecules can only lead to a slightly delocalized character of the excitation over both types of pigments. Excitations are probably to some extent delocalized over several Chl *a* pigments. Therefore, Förster transfer from Chl *b* to Chl *a* can take place towards excitonically coupled Chl *a* pigments. However, the presence or absence of this coupling hardly influences the transfer rate from Chl *b* to Chl *a* as long as the Förster overlap integral between the Chl *b* fluorescence and the absorption spectra of the individual or excitonically coupled Chl *a* pigments does not largely differ [28], which is the case for LHCII. Therefore, it seems justified to discuss energy transfer from Chl *b* to Chl *a* in terms of the Förster mechanism. However, one should keep in mind that in the equation given by Förster (see below), fluorescence spectra are used of molecules which are equilibrated in the excited state. Since vibrational equilibration may occur on a time scale of a few hundreds of femtoseconds the calculated rates could be slightly in error. The effect is expected not to be large for pigments with a small Huang–Rhys factor [21] which most likely prevail in LHCII (see also Ref. [10]). Also the dipole–dipole approximation that is used in the derivation of the Förster formula might not be entirely justified for distances between pigments of 0.9 nm although the introduced error is probably small [29]. We will therefore treat energy transfer in LHCII by the standard Förster approach, in which the rate k_{DA} from a donor molecule D to an acceptor molecule A falls off with the sixth power of distance between D and A:

$$k_{DA} = \kappa^2 k_{rad} (R_0/R)^6.$$

Here, κ^2 is an orientation factor, with possible values from 0 to 4 (see Appendix). k_{rad} is the radiative rate of the donor molecule in the absence of energy transfer, being $(23\ ns)^{-1}$ and $(15\ ns)^{-1}$ for Chl *b* and Chl *a*, respectively. R_0 is called the Förster radius, and contains the overlap integral of donor emission and acceptor absorption. It is strongly dependent on the refractive index *n* of the medium surrounding donor and acceptor, as is apparent from its definition, given in the Appendix. A range of different values for R_0 has been published over the years (see e.g. Ref. [30]). These values were usually determined from room temperature measurements on Chl in solution. The spread in the values is contributed to by the variation in n. In the Appendix we estimate R_0 for Chl *b* to Chl *b*, Chl *b* to Chl *a* and Chl *a* to Chl *a* transfer for LHCII at 77 K as a function of the separation between the absorption and fluorescence peaks. We find as transfer rates

$$k_{DA} = \frac{C}{n^4} \kappa^2 (1/R)^6.$$

Where *C* is 162, 54.6 and 79.3 ps^{-1} for Chl *a* → Chl *a*, Chl *b* → Chl *a* and Chl *b* → Chl *b* transfer respectively. *R* is taken in nm. Thus, with $n = 2.0$, $R = 1.0$ nm and $\kappa^2 = 1$, one finds a transfer time of 0.29 ps from Chl *b* to Chl *a*.

Although Chl *a* and Chl *b* cannot be discriminated in the present 3.4 Å resolution structure of LHCII, an assignment of the pigments has been made, with the 7 chlorophylls closest to the two central luteins being Chl *a* and the more peripheral ones being Chl *b* [3]. This arrangement and assignment of the pigments in a monomer of LHCII is shown in Fig. 7. In this assignment, for each Chl molecule two orientations for the Q_y transition dipole moment are possible: either along NA and NC (here denoted as AC) or along NB and ND (here denoted as BD (notation of NA, NB, NC and ND refers to the nomenclature of the nitrogens in the porphyrin rings in the crystal structure). In the following, we will use this assignment and first consider the transfer rate from each Chl *b* to its closest Chl *a* neighbor, for all four possible relative orientations. The real transfer rate from any Chl molecule will be faster than this first approximation due to additional transfer to Chl molecules further away. However (see Fig. 7), apart from Chl *b6*, all Chl molecules have one neighboring Chl *a* molecule that is by far closest, and such an approach will yield reasonable results in view of the strong distance (R^{-6}) dependence of the employed Förster energy-transfer mechanism. In Ref. [4] it was demonstrated that if one takes the Chl *a* and Chl *b* assignment of Kühlbrandt et al. [3], for some pigments the Q_y can only be directed along AC or BD, since otherwise one would

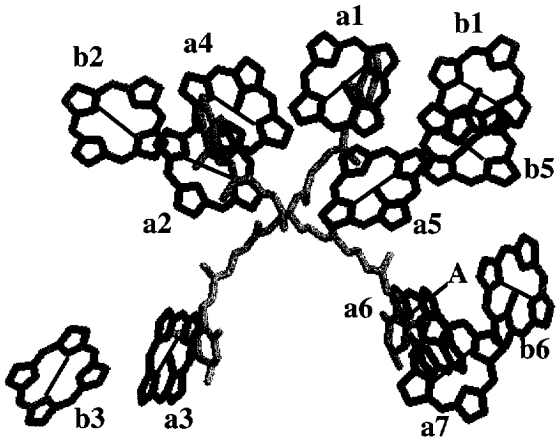

Fig. 7. Arrangement of the pigments in a monomer of LHCII. Black: Chl *a*. Dark grey: Chl *b*. Light grey: luteins. The numbering and assignment of the chlorophylls follows Ref. [3], in which work these data were first presented. The lines through the center of the molecules connect NA and NC, the AC direction in the text. The A indicates the position of NA in Chl *a6*. From model calculations on energy transfer within the monomeric LHCII complex using this structure and assignment, we conclude that transfer from Chl *b2*, *b3* and *b6* to Chl *a* is sub-picosecond. Equilibrium between the pairs *a1* and *a2* and *a6* and *a7* is estimated to take a few picoseconds. Due to projection, *a1* and *a2* and *a4* and *a5* do not appear as pairs in this figure. The slowest process (~ 10 ps) is thought to be equilibration of *a3* with the other Chl *a* molecules, see text. The figure was created using the program RasMol2.4.

get a linear dichroism and/or circular dichroism spectrum that would be completely in disagreement with the experimental spectra. It was concluded that for Chl *a5* and *a7* the Q_y transition dipole moment is oriented along AC whereas for Chl *b3* it is oriented along BD. For Chl *a1* and *a4* it is very likely to be oriented along AC. Given the most perfect C_2 symmetry for 6 Chl *a* molecules one might suspect that the orientation of Chl *a2* is symmetry related to that of Chl *a5* (along AC). Moreover, Chl *a3* and Chl *a6* are probably symmetry related but it is unknown whether Q_y is oriented along AC or BD. Apart from Chl *b3*, nothing is known about the orientation of the Chl *b* molecules.

From Table 2 the relative rates for transfer from Chl *b* to Chl *a* can be deduced. Taking a value on $n = 2.5$ the listed values have to be multiplied with a factor of 1.4 in order to arrive at transfer rates in ps^{-1}. Irrespective of the particular choices for the relative orientations of the pigments one arrives at transfer times between several hundreds of femtoseconds and one picosecond for transfer from chlorophylls *b2*, *b3* and *b6*. Note that transfer from Chl *b6* takes place to both Chl *a6* and *a7*. If for a particular orientation of Chl *b6* the transfer to one of these two is unfavorable then the transfer to the other is favorable. According to this table, energy transfer from Chl *b1* or *b5* is not faster than several hundreds of femtoseconds for $n = 2.5$. Therefore, this indicates that n is not larger than 2.5 since otherwise even the transfer rates between pigments that are very close together becomes to slow to explain the fast transfer kinetics. This in turn implies that the transfer times from Chl *b2*, *b3* and *b6* are always less than one picosecond and thus that the slow transfer time from Chl *b* to Chl *a* can only be due to either Chl *b1* or *b5*. It should be stressed that the presented smallest transfer rates give upper limits for the life times of the excitations on the particular Chl *b* pigments since for these small rates transfer will also take

Table 2
Values for κ^2/R^6 compared

#b, #a	*R*	AC AC	AC BD	BD AC	BD BD
1, 1	1.1	0.90	*0.17*	0.039	*1.2*
2, 2	0.84	2.1	*1.9*	2.1	*0.94*
3, 3	0.92	*0.38*	0.70	*2.1*	0.78
5, 5	0.89	2.1	*0.044*	0.15	*2.1*
6, 6	0.88	0.20	1.3	3.8	0.61
6, 7	1.0	0.70	*0.90*	1.7	*0.025*

In this table we compare the value for κ^2/R^6 for the five Chl *b*–Chl *a* pairs for all four possible orientations. AC indicates that the Q_y transition is along the line N_A–N_C, BD that the Q_y transition is perpendicular to that, along the line N_B–N_D. Left position in the first column indicates Chl *b*, right position Chl *a*. Numbering of the chlorophylls follows Ref. [3]. *R* is the distance between Mg atoms of the Chl and is taken in nm. Values in italic correspond to relative orientations that seem to be in conflict with present assignments, see text.

place via other pigments but the transfer can still take several picoseconds. Therefore, our measurements do not contradict the assignment of the chlorophyll identities by Kühlbrandt and coworkers [3].

Based on an average transfer time of 500 fs from Chl *b* to Chl *a* and taking a value of $\kappa^2 = 1$, Pålsson et al. [15] arrived at average closest distances between Chl *b* and Chl *a* molecules of 1.3–1.4 nm. According to our calculations this corresponds to a refractive index of $n = 1.5$. Based on our time-resolved measurements we cannot make a choice between the proposal of Kühlbrandt et al. ([3], shown in Fig. 7) and Pålsson et al. ([15], Chl *b* and Chl *a* are in different layers) since the transfer rates depend so heavily on the (yet unknown) value(s) of the refractive index which might be large because of the high pigment content in LHCII (30% of mass).

We have also calculated transfer rates between Chl *a* molecules. Taking the largest reasonable value for the refractive index, $n = 2.5$, we arrive at an equilibration time between Chl *a1* and *a2* of at most 1 ps, irrespective of the chosen orientations. The same holds for equilibration between Chl *a4* and *a5*. Taking the orientations of the transition dipole moment along the AC axis (see argumentation above) this time reduces in both cases to 600 fs. The equilibration between the pairs *a1* and *a2* and *a6* and *a7* takes about 5 ps. In determining these times, we assumed that forward and backward transfer are approximately equally fast. If this is not the case these rates will slow down somewhat. Taking the orientation of Q_y in Chl *a7* along the *X* axis (see above) it can similarly be calculated that equilibration between Chl *a6* and *a7* takes at most 1 ps. There is a striking long-lived component (close to 14 ps) observed in our measurements, which corresponds to the long-lived shoulder near 670 nm that is excited after excitation at 649 and 661 nm. A similar lifetime turned out to reflect an equilibration process in the Chl *a* pool of LHCII at 12 K [16]. Assuming that all monomeric subunits of LHCII have similar optical properties such a slow lifetime can only be explained if the Q_y of Chl *a3* is oriented along the BD axis, where we have used the fact that the refractive index is probably not larger than 2.5. The slow (> 10 ps) Chl *a* equilibration then corresponds with equilibration of *a3* with the other Chl *a* molecules.

For illustration purposes we have stimulated the equilibration process in monomeric LHCII using the three expressions for the Förster transfer as given in the Appendix. The refractive index was taken to be 2.5. We neglected spectral differences between various Chl *a* (or Chl *b*) molecules. The orientations of the Q_y transition dipole moments were somewhat arbitrarily taken along the BD axis for the Chl *b* molecules. The exact choice may have a significant effect on the transfer from Chl *b1* and *b5* (see above) and therefore we will predominantly comment here on the processes that take place after Chl *b* to Chl *a* transfer has occurred. For Chl *a1, a2, a4, a5* and *a7* the transition dipoles are put along AC, whereas for Chl *a3* it is put along BD, as explained above. Because of the quasi C_2 symmetry in monomeric LHCII we also put the transition dipole of *a6* along BD.

To study the flow of energy we selectively placed excitations on each of the Chl *b* molecules and inspected which processes took place. The dominant transfer processes from Chl *b* to Chl *a* take place with time constants between 300 and 700 fs and a slower phase of 4 ps is observed. However, the choice of the transition dipole moment directions for Chl *b1* and Chl *b5* can especially influence (i.e. speed up) the slowest process. Equilibration between the Chl *a* molecules in the upper layer (assignment as in Ref. [3]) takes place within 800 fs. Equilibration of Chl *a3* with the rest of the monomer takes 10 ps, whereas equilibration between Chl *a6* and Chl *a7* and the upper layer occurs with a time constant of 5 ps. We have not done extensive calculations on equilibration processes within the entire trimer but it seems that transfer between monomers occurs on a time scale slower than 10 ps and it appears to be of the right order of magnitude to explain the time scale of the annihilation processes (10–20 ps).

In conclusion, the majority of the kinetic processes that we observed for LHCII on a time scale from ~ 100 fs to ~ 20 ps can be described reasonably well with the Förster formalism, given the assignment of the chlorophyll identities by Kühlbrandt and coworkers [3] and the transition dipole moment orientations that were derived by Gülen et al. [4]. Note however, that this agreement only holds if the value of the refractive index has at least a value close to 2 but preferably closer to 2.5.

Whether this is indeed a realistic value has to be determined in the future. Irrespective of the value of the refractive index, the variation in Chl–Chl distances in any assignment of Chl identities and transition dipole moment orientations must lead to a multitude of time constants in the equilibration process, as we indeed experimentally observed. This "structural disorder" in LHCII contrasts with the high symmetry observed in the recently obtained structure of the peripheral bacterial antenna, LH-II [31], and possibly the core LH-I complex as well [32]. In modelling the equilibration between LHCII and other antenna complexes and finally, the reaction center, the observed multitude of equilibration lifetimes within the LHCII complex will form a complicating factor.

Acknowledgements

This research was supported through EEC contracts No. CT 92 0796 and CT 93 0278. We would like to acknowledge Dr. W. Kühlbrandt for sending us the coordinates of the pigments in LHCII, Professor W. Struve for sending his manuscript prior to publication, and R. Monshouwer and A. Baltuska for expert assistance in using the Ti:sapphire setup. Financial support came from the Dutch science foundations FOM en SLW.

Appendix A

To calculate Förster rates we used the following expression (for a recent treatment of Förster energy transfer see e.g. Ref. [33]):

$$k_{DA} = (k_{rad})(R_0/R)^6.$$

Here k_{DA} is the rate of energy transfer from a donor molecule to an acceptor molecule, k_{rad} is the rate of the radiative decay and R denotes the distance between the centers of the pigments (in nm). R_0 is the Förster radius which is defined as

$$R_0^6 = C\kappa^2 n^{-4}\left(\int F_D(\nu)\,\varepsilon_A(\nu)\,\nu^{-4}\,d\nu\right).$$

$C = 0.716 \times 10^{18}$, n is the refractive index, κ^2 is a factor which depends on the mutual orientation of the donor and acceptor molecule and it can vary between 0 and 4. Its definition is given below. F_D denotes the fluorescence spectrum of the donor molecule and its area is normalized to unity on a frequency scale; ε_A is the molar extinction coefficient (in M^{-1} cm^{-1}) of the acceptor molecule and ν is the frequency in s^{-1}. The definition of κ is as follows:

$$\kappa = \cos(\hat{\mu}_D\hat{\mu}_A) - 3\left[\cos(\hat{\mu}_D\hat{R}_{DA})\right]\left[\cos(\hat{\mu}_A\hat{R}_{DA})\right].$$

Here μ_D and μ_A denote the normalized transition dipole moment vectors of the donor and acceptor molecules, whereas R_{DA} is a normalized vector between the centers of the donor and acceptor molecule. κ can take values from -2 to 2.

In order to calculate Förster rates in LHCII at 77 K, reasonable estimates are needed for the absorption and fluorescence spectra of the different Chl *a* and Chl *b* molecules. The fluorescence spectrum of LHCII at 77 K stems exclusively from Chl *a* and we used it as an approximation of the Chl a fluorescence spectrum. The approximate shape of the absorption spectrum of Chl *a* was calculated from the fluorescence spectrum using the Stepanov relation [34]. Since absorption and fluorescence spectra of individual pigments in LHCII can differ, the value of the overlap integral in the above equation was calculated for various differences between the positions of the absorption and emission maxima. The calculated values are given below. The overlap integral has been normalized to one for the case that the maxima of absorption and fluorescence spectra coincide. The absolute value of the molar extinction coefficient was approximated as follows. The absorption spectrum of Chl *a* was measured at room temperature both in methanol and in 80% acetone where the molar extinction coefficients are well known [35]. Since the calculated absorption spectrum of Chl *a* in LHCII at 77 K is much narrower than the measured spectra at room temperature but the dipole strength is probably very similar we normalized the areas of the calculated and measured spectra with respect to each other in the Q_y region (approximately above 640 nm). The areas were almost identical for methanol and 80% acetone. This calculation led to a molar extinction coefficient ε_A of 140 000 M^{-1} cm^{-1} in the maximum. Note that the sharpening of the absorption spectrum upon cooling has led to an increased extinction coefficient. These results

Table 3
Relative overlap integral for various energy differences between donor and acceptor

$\lambda_A - \lambda_D$ (nm)	Overlap
−8	0.28
−6	0.46
−4	0.68
−2	0.88
0	1.00
2	1.01
4	0.97
6	0.89
8	0.82
10	0.75
12	0.69
14	0.64
16	0.59
18	0.54
20	0.49
22	0.45
24	0.41
26	0.39
28	0.37

lead to the following expression for transfer between two Chl *a* molecules if the maxima of absorption and fluorescence coincide $k_{DA} = (\tau_{rad})^{-1}\kappa^2 n^{-4}(11.6/R)^6$, where R is expressed in nm. Taking τ_{rad} to be 15 ns [36] leads to $k_{DA} = 162.4n^{-4}\kappa^2 R^{-6}$, where k is expressed in ps^{-1}. If the emission maximum of the donor molecule is shifted more to the blue, the transfer rate changes according to the changing overlap integral as indicated in Table 3.

Since we are not able to measure the fluorescence from Chl *b* in LHCII we simply approximated the shape of this spectrum by that of Chl *a* and consequently the shape of the absorption spectra of Chl *a* and Chl *b* were also assumed identical. The transfer rate from Chl *b* to Chl *a* is now calculated to be $k_{DA} = 54.6n^{-4}\kappa^2 R^{-6}$ taking a radiative lifetime of 23 ns [36] and a difference of 22 nm between the absorption maximum of Chl *a* and the emission maximum of Chl *b*. Note that the transfer rates are not particularly sensitive to the exact positions of the absorption and fluorescence maxima (see Table 3).

The transfer rate between Chl *b* molecules can only be calculated after making a reasonable choice for the value of the molar extinction coefficient of Chl *b*. The extinction coefficient scales with the dipole strength and thus with the inverse of the radiative lifetime. This leads to a reduction of the overlap integral with a factor 23/15 = 1.53 (ratio of radiative lifetimes of Chl *b* and Chl *a*) as compared to that for transfer from Chl *b* to Chl *a*. Taking the maxima of the absorption and the emission spectrum at the same wavelength, we find $k_{DA} = 79.3n^{-4}\kappa^2 R^{-6}$.

References

[1] W. Kühlbrandt and D.N. Wang, Nature (London) 350 (1991) 130.
[2] D. Siefermann-Harms, Physiol. Plantarum. 69 (1987) 561.
[3] W. Kühlbrandt, D.N. Wang and Y. Fujiyoshi, Nature (London) 367 (1994) 614.
[4] D. Gülen, R. van Grondelle and H. van Amerongen, in: Photosynthesis: from light to biosphere, Proc. Xth Intern. Photosynthesis Conf., Vol. I, ed. P. Mathis (Kluwer, Dordrecht, 1995) p. 335.
[5] P.W. Hemelrijk, S.L.S. Kwa, R. van Grondelle and J.P. Dekker, Biochim. Biophys. Acta 1098 (1992) 159.
[6] S. Krawczyk, Z. Krupa and W. Maksymiec, Biochim. Biophys. Acta 1143 (1993) 273.
[7] S. Nussberger, J.P. Dekker, W. Kühlbrandt, B.M. van Bolhuis, R. van Grondelle and H. van Amerongen, Biochemistry 33 (1994) 14775.
[8] H. van Amerongen, S.L.S. Kwa, B.M. van Bolhuis and R. van Grondelle, Biophys. J. 67 (1994) 837.
[9] E.J.G. Peterman, J.P. Dekker, R. van Grondelle, H. van Amerongen and S. Nussberger, Lith. J. Phys. 34 (1994) 301.
[10] N.R.S. Reddy, H. van Amerongen, S.L.S. Kwa, R. van Grondelle and G.J. Small, J. Phys. Chem. 98 (1994) 4729.
[11] D.D. Eads, E.W. Castner, R.S. Alberte, L. Mets and G.R. Fleming, J. Phys. Chem. 93 (1989) 8271.
[12] S.L.S. Kwa, H. van Amerongen, S. Lin, J.P. Dekker, R. van Grondelle and W.S. Struve, Biochim. Biophys. Acta 1102 (1992) 202.
[13] C.W. Mullineaux, A.A. Pascal, P. Horton and A.R. Holzwarth, Biochim. Biophys. Acta 1141 (1993) 23.
[14] M. Du, X. Xie, L. Mets and G.R. Fleming, J. Phys. Chem. 98 (1994) 4736.
[15] L.O. Pålsson, M.D. Spangfort, V. Gulbinas and T. Gillbro, FEBS Letters 339 (1994) 134
[16] T. Bittner, K.-D. Irrgang, G. Renger and M.R. Wasielewski, J. Phys. Chem. 98 (1994) 11821.
[17] T. Bittner, G.P. Wiederrecht, K.-D. Irrgang, G. Renger and M.R. Wasielewski, Chem. Phys. 194 (1995) 311.
[18] S. Savikhin, H. van Amerongen, S.L.S. Kwa, R. van Grondelle and W.S. Struve, Biophys. J. 66 (1994) 1597.

[19] F.J. Kleima, H.M. Visser, R. van Grondelle and H. van Amerongen, in: Photosynthesis: from light to biosphere, Proc. Xth Intern. Photosynthesis Conf., Vol. I, ed. P. Mathis (Kluwer, Dordrecht, 1995) p. 57.
[20] E.J.G. Peterman, F.M. Dukker, R. van Grondelle and H. van Amerongen, Biophys. J. 69 (1995) 2670.
[21] W.S. Struve, Biophys. J. 69 (1995) 2739.
[22] H.M. Visser, M.-L. Groot, F. van Mourik, I.H.M. van Stokkum, J.P. Dekker and R. van Grondelle, J. Phys. Chem. 99 (1995) 15304.
[23] I.H.M. van Stokkum, T. Scherer, A.M. Brouwer and J.W. Verhoeven, J. Phys. Chem. 98 (1994) 852.
[24] H. van Amerongen and W.S. Struve, J. Phys. Chem. 95 (1991) 9020.
[25] R.L. van Metter, Biochim. Biophys. Acta 462 (1977) 642.
[26] J.F. Shepanski and R.S. Knox, Isr. J. Chem. 21 (1981) 325.
[27] D. Gülen and R.S. Knox, Photobiochem. Photobiophys. 7 (1984) 277.
[28] H. van Amerongen and W.S. Struve, J. Lumin. 51 (1992) 29.
[29] D.E. LaLonde, J.D. Petke and G.M. Maggiora, J. Phys. Chem. 92 (1988) 4746.
[30] R.S. Knox, in: Bioenergetics of photosynthesis, ed. Govindjee (Academic Press, New York, 1975) p. 183.
[31] G. McDermott, S.M. Prince, A.A. Freer, A.M. Hawthornthwaite-Lawless, M.Z. Papiz, R.J. Cogdell and N.W. Isaacs, Nature 374 (1995) 517.
[32] S. Karrasch, P.A. Bullough and R. Ghosh, EMBO J. 14 (1995) 631.
[33] W.S. Struve, in: Anoxygenic photosynthetic bacteria, eds. R.E. Blankenship, M.T. Madigan and C.E. Bauer (Kluwer, Dordrecht, 1995) pp. 297–313.
[34] B.I. Stepanov, Soviet Phys. Dokl. 2 (1957) 81.
[35] R.J. Porra, W.A. Thompson and P.E. Kriedemann, Biochim. Biophys. Acta 975 (1989) 384.
[36] G.R. Seely and J.S. Connolly, in: Light emission by plants and bacteria, eds. Govindjee, J. Amesz and D.C. Fork (Academic Press, New York, 1986) p. 99.